

Component Integration Strategies In Metamorphic 4-junction III-V Concentrator Solar Cells

Iván García , John F. Geisz , Ryan M. France
Myles A. Steiner , Daniel J. Friedman

Abstract. Progressing beyond 3-junction inverted-metamorphic multijunction solar cells grown on GaAs substrates, to 4-junction devices, requires the development of high quality metamorphic 0.7 eV GaInAs solar cells. Once accomplished, the integration of this subcell into a full, monolithic, series connected, 4J-IMM structure demands the development of a metamorphic tunnel junction lattice matched to the 1eV GaInAs subcell. Moreover, the 0.7 eV junction adds about 2 hours of growth time to the structure, implying a heavier annealing of the subcells and tunnel junctions grown first. The final 4J structure is above 20 μm thick, with about half of this thickness used by the metamorphic buffers required to change the lattice constant throughout the structure. Thinning of these buffers would help reduce the total thickness of the 4J structure to decrease its growth cost and the annealing time. These three topics: development of a metamorphic tunnel junction for the 4th junction, analysis of the annealing, and thinning of the structure, are tackled in this work. The results presented show the successful implementation of an antimonide-based tunnel junction for the 4th junction and of pathways to mitigate the impact of annealing and reduce the thickness of the metamorphic buffers.

INTRODUCTION

Experimental efficiencies over 42% percent have been published for 3-junction inverted metamorphic (3J-IMM) multijunction solar cells [1]. Adding a 4th 0.7 eV junction, the theoretical efficiency potential increases by over 4%. Currently, 4-junction inverted metamorphic (4J-IMM) multijunctions solar cells are under development, with efficiencies over 48% foreseen in the short term [2]. The structure shown in figure 1 offers a near-optimum efficiency potential for operation under terrestrial direct spectrum. Outstanding performance Ga_{0.47}In_{0.53}As (0.7 eV bandgap) metamorphic solar cells, grown on GaAs substrates with a total lattice-mismatch of around 4%, have been developed [2,3]. However, the integration of all components into a full 4J multijunction solar cell structure brings about a set of growth-related issues that need to be addressed. Firstly, an additional tunnel junction must be developed to series-connect the 4th junction with minimum optical and electrical losses. Second, the integration of the 4th junction into the 3J structure involves around 2 hours of additional growth with the associated thermal load to the structure. Thirdly, the total thickness of the resulting structure is over 20 μm , half of it coming from the buffer structures required to grade the lattice constant of the metamorphically-grown materials. In this work we

first present a metamorphic tunnel junction developed for the integration of the 4th junction in a 4J structure. Then we analyze the effect of the annealing on the performance of the subcells and tunnel junctions in the 4J structure. Finally, we present the results about the ongoing research aiming to reduce the total thickness of the metamorphic buffers while preserving the performance of the subcells.

EXPERIMENTAL

The semiconductor structures are grown by metal-organic vapor-phase epitaxy (MOVPE) in a custom-built, atmospheric-pressure, vertical reactor, using AsH₃, PH₃, TMGa, TMIIn, TMAI as main constituent precursors and DEZn, H₂Si₄, H₂Se and CCl₄ as precursors for the dopants. The structures are processed into solar cell devices using standard photolithographic techniques and gold electroplating as metal deposition method. Anti-reflection coatings (ARC) are deposited on some of the devices studied in this work, and consist on standard MgF₂/ZnS bi- and tri- layer stacks. In-situ curvature and ex-situ X-Ray diffraction are used to assess the strain evolution and structural quality of the metamorphic structures. The solar cells are characterized using external and internal quantum efficiency (EQE and IQE), dark and spectrally-corrected 1-sun IV curves, electro-

luminescence (EL) and flash-based concentration measurements.

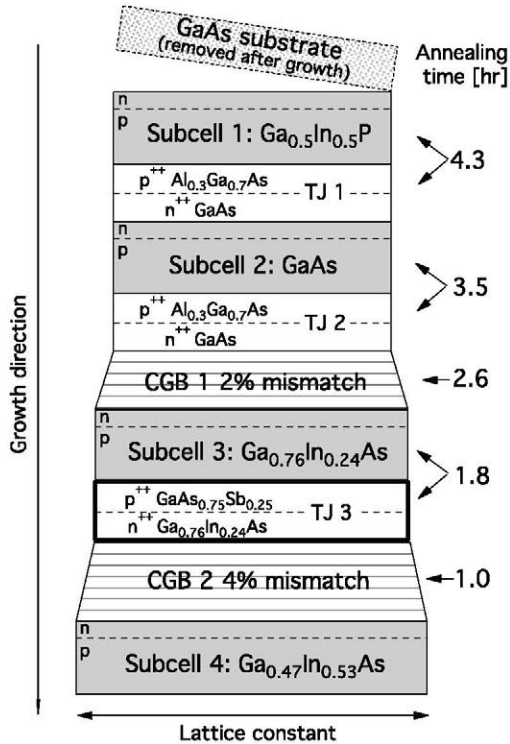


FIGURE 1. General structure of the 4J solar cells under development. The list on the right indicates the annealing time each component is submitted to during growth. The annealing temperature is ~ 675 C for most of the growth time. The drawing is not to scale.

METAMORPHIC TUNNEL JUNCTION

In our 3J-IMM solar cell designs, the tunnel junctions were grown lattice matched to the GaAs substrate and were based on AlGaAs/GaAs heterostructures [4]. The TJ connecting the GaAs(2nd) and GaInAs(3rd) subcells is grown before the metamorphic buffer since it was found out that, for the growth conditions used, the quality of the n-type doped buffers is better than when using p-type dopants such as Zn. For the 4J-IMM design, the TJs connecting the 1st/2nd and 2nd/3rd junctions are the same as in the 3J-IMM design, except for one important change discussed in the next section; an additional TJ is required to connect the 3rd and 4th junctions. For the same reason, this TJ is grown before the 2nd metamorphic buffer, used to grade the lattice constant to the $\text{Ga}_{0.47}\text{In}_{0.53}\text{As}$ material (see figure 1). Therefore, it was required to develop a metamorphic TJ lattice matched to the $\text{Ga}_{0.76}\text{In}_{0.24}\text{As}$ material.

Among the set of ternary and quaternary materials that can be grown lattice matched to $\text{Ga}_{0.47}\text{In}_{0.53}\text{As}$, all In-containing options were discarded given the well-known difficulties in using carbon to dope these materials. The (Al)GaAsSb material was deemed as the most appropriate choice, since, in addition to allowing high carbon doping levels, the (Al)GaAsSb/GaInAs heterostructure band alignment is reported to be type-II, which facilitates the tunneling of carriers [5]. Moreover, GaAsSb lattice-matched to $\text{Ga}_{0.76}\text{In}_{0.24}\text{As}$ is transparent to the light that has to reach the 4th junction. We therefore developed $\text{GaAs}_{0.75}\text{Sb}_{0.25}\text{C}/\text{Ga}_{0.76}\text{In}_{0.24}\text{As}:\text{Se}$ TJ structures.

The main challenges envisaged to be going to face were the reportedly complex growth of the metastable GaAsSb material and, moreover, its metamorphic growth on the rough surface of the metamorphic buffer [1]. Although there is extensive literature about the successful growth of good quality GaAsSb layers and GaAsSb/GaInAs tunnel junctions [5,6], their growth on metamorphic structures with the in-plane lattice constant of 1eV $\text{Ga}_{0.76}\text{In}_{0.24}\text{As}$ has not been reported.

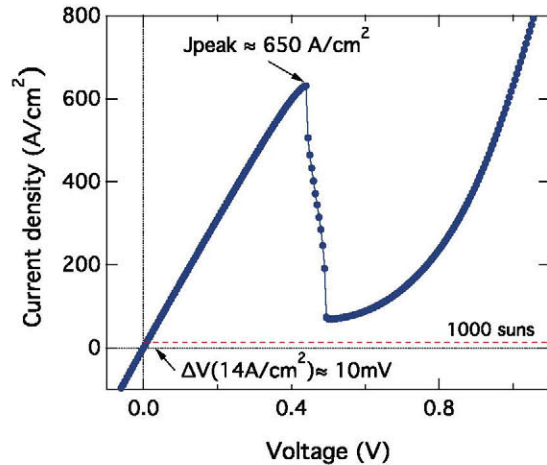


FIGURE 2. J-V curve of the $\text{GaAs}_{0.75}\text{Sb}_{0.25}\text{C}/\text{Ga}_{0.76}\text{In}_{0.24}\text{As}:\text{Se}$ developed.

A paper with a detailed description of the TJ growth is in preparation. Here we focus on the performance results of the TJ developed. In figure 2 the IV-curve of one such TJs developed is shown. A peak current density over 650 A/cm^2 is obtained, well over the $\sim 14 \text{ A/cm}^2$ required for operation of the 4J device at 1000 suns. The voltage drop across the TJ at 14 A/cm^2 is less than 10 mV and therefore the electrical losses introduced by this TJ are negligible. Moreover, the insertion of this TJ in the 4J structure was found not to affect the performance of the $\text{Ga}_{0.47}\text{In}_{0.53}\text{As}$ 4th junction. Its carrier collection efficiency and recombination current, measured by QE and dark IV curves respectively (not included here for

brevity), do not show any significant change after inserting the TJ in the structure.

EFFECT OF ANNEALING

The first subcells and tunnel junctions grown in the 4J cell are subjected to a heavy thermal load during growth of the subsequent components of the structure, as shown in figure 1. We studied the effect of this annealing in order to determine if it could be hindering the performance of the 4J and to take the corresponding corrective measures. The first 4J structures developed showed evidence of annealing effect by a TJ failing at low concentrations. To isolate the TJs and determine which one was failing, a set of two-junction (2J) cells was grown, consisting of the 1st/2nd, 2nd/3rd and 3rd/4th junctions of the 4J-IMM. For each case, half the sample was processed into solar cells as grown, and the other half was submitted to exactly the same annealing they would be submitted to in a 4J-IMM structure, and then they were also processed into solar cells. We surprisingly found that the TJ failing was the 2nd. This TJ is virtually identical to the 1st one, consisting of a AlGaAs:C(20nm)/GaAs:Se(12nm) structure with identical surrounding layer doping levels and dopants used, and it is annealed for half an hour less (see figure 1). Therefore, it was puzzling why this TJ had a lower strength against annealing than TJ1 and, therefore, the redesign to tackle was not clear.

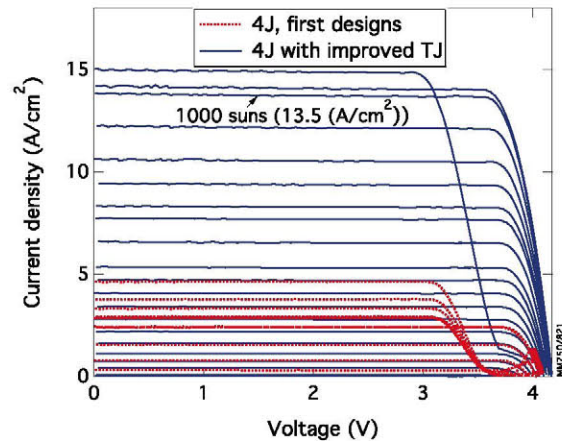


FIGURE 3. Concentrator J-V curves of the 4J-IMM solar cells with the tunnel junctions developed.

In TJ1 a thin GaAs:Se cathode (around 12 nm) is used to minimize the optical absorption between the 1st and 2nd subcells. However, such a thin cathode is not required in TJ2 on optical absorption grounds, given the lower bandgap of the 3rd subcell (around 1eV) and the fact that the 2nd GaAs subcell is designed to be optically thick. It was observed that when the TJ2 cathode was thickened, its tunneling current increased.

When thickened to 25 nm, this TJ did not limit the performance of the 4J structures up to above 1000 suns. The exact reason for this is not known, but an expectable drift of the growth conditions and growth environment along the growth of the 4J structure could lead to different dopant incorporation, thickness, etc, that could make TJ2 weaker. In figure 3, concentration JV curves of 4J solar cells before and after redesigning the 2nd TJ are shown. Note that these 4J cells include the antimonide-based TJ presented in last section. As can be seen, no TJ in the structure is limiting the performance of the 4J-IMM solar cell up to concentrations over 1000 suns.

The 2J structures presented above were also used to determine if annealing affects the subcell performance. Surprisingly, as an overall conclusion of this study, the subcells performance does not change noticeably after annealing: the quantum efficiency (QE), dark IV currents and series resistance (derived from flash measurements) do not change for operation at 1-sun or under concentration (see figure 4). However, interestingly, for the low irradiance levels used normally to take QE measurements, we found a curious effect consisting of an apparent deterioration of the annealed Ga_{0.5}In_{0.5}P top cells QE response. Moreover, this effect was observed only in high-performance top cell designs with thick emitters (p-n junction placed at the back of the solar cell) [6]. When these top cells are light-biased with irradiances of just 0.1 suns during the QE measurements, their QE fully recovers. The reasons of this effect are unknown but its dependence on the thickness of the n-type GaInP emitter suggests that it could be due to traps in this material, which are passivated with the carrier injection from the light bias. At any rate, this effect is only important as far as the QE measurement of these solar cells at very low light bias is concerned, but does not affect their performance at 1-sun or concentration.

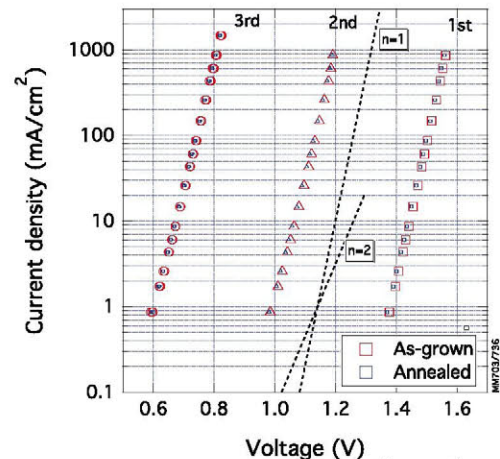


FIGURE 4. Dark IV curves of the 1st, 2nd and 3rd subcells of the 4J structure, before and after annealing. These curves were obtained using the EL technique.

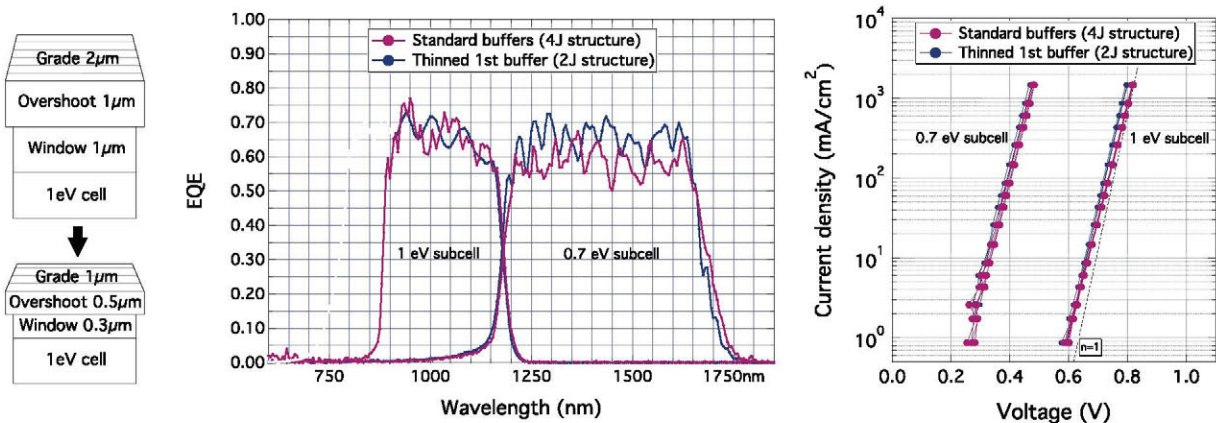


FIGURE 5. EQE and dark IV of the 3rd and 4th junctions with standard and thinned 1st buffer. The junctions are in a 4J and a 3rd/4th subcells 2J structure, respectively, which explains the difference in the cut-on wavelength of the 1eV cell EQE.

METAMORPHIC BUFFER THINNING

A close look at the high-performance 4J-IMM structures and growth routines developed reveals that around 50% of the total thickness (~ 22 μm) and around 40% of the total growth time is taken by the metamorphic buffers used (see figure 1). Therefore, it is desirable to decrease the thickness of the metamorphic buffer in order to reduce the growth cost and, additionally, the thermal load to which the top subcells and tunnel junctions are subjected.

Previously we developed a design for the 1st buffer that allowed us to thin the compositionally graded layer from 2 to 1 μm by reorganizing the relaxation dynamics using a misfit step jump at the beginning of its growth [7]. Here we present the results of reducing also the thickness of the overshoot and window layers of the buffer structure so that its total thickness is 1.8 μm, representing a total reduction in buffer thickness of 2.2 μm. As observed in figure 5, this new thinned buffer allows the growth of 1eV and 0.7eV subcells with no significant impact on the carrier collection efficiency and recombination currents, which is the ultimate expression of a good photovoltaic quality in the thinned metamorphic buffer.

CONCLUSIONS

The integration of a 0.7 GaInAs subcell into a 3J-IMM to develop a 4J-IMM has been successfully accomplished by development of a metamorphic GaAsSb-based TJ and by redesigning the 2nd TJ, which was affected by the thermal annealing added by the growth of the 0.7 eV junction. Ongoing work on thinning the metamorphic buffers has so far enabled the reduction of the total thickness of the 4J-IMM

structure by 2.2 μm without significantly affecting the performance of the metamorphic junctions.

ACKNOWLEDGEMENTS

The authors thank W. Olavarria and M. Young for growth and fabrication of structures, and W. E. McMahon for useful discussions. I. Garcia holds an IOF grant from the People Programme (Marie Curie Actions) of the European Union's Seventh Framework Programme (FP7/2007-2013) under REA grant agreement No. 299878. This work is supported by the U.S. Department of Energy under Contract No. DE-AC36-08-GO28308 with the National Renewable Energy Laboratory.

REFERENCES

1. R. M. France, J. F. Geisz, M. A. Steiner, D. J. Friedman, J. S. Ward, J. M. Olson, W. Olavarria, M. Young, A. Duda, *IEEE J. Photovolt.* **3**, pp. 893-898 (2013).
2. R. M. France, W. E. MacMahon, A. G. Norman, J. F. Geisz, I. Garcia, M. A. Steiner, D. J. Friedman, *submitted to this conference*.
3. R. M. France, I. Garcia, W. E. McMahon, A. G. Norman, J. Simon, J. F. Geisz, D. J. Friedman, M. J. Romero, *IEEE J. Photovolt.*, **4**, pp. 190-195 (2014).
4. J.F. Geisz, S. Kurtz, M. W. Wanlass, J. S. Ward, A. Duda, D. J. Friedman, J. M. Olson, W. E. McMahon, T. E. Moriarty, J. T. Kiehl, *Appl. Phys. Lett.* **91**, 023502 (2007)
5. N. Suzuki, T. Anan, H. Hatakeyama, M. Tsuji, *Appl. Phys. Lett.* **88**, 231103 (2006).
6. U. Seidel, H.-J. Schimper, Z. Kollonitsch, K. Moller, K. Schwarzburg, T. Hannapel, *J. Crys. Growth* **298**, pp. 777-781 (2007).
7. J. F. Geisz, M. A. Steiner, I. Garcia, S. R. Kurtz, D. J. Friedman, *Appl. Phys. Lett.*, **103**, 041118 (2013)
8. I. Garcia, R. M. France, J. F. Geisz, J. Simon, *J. Crys. Growth*, **393**, pp. 64-69 (2014).